ACS Pharmacology & Translational Science

pubs.acs.org/ptsci

Article

Development of Noninvasive Activity-Based Protein Profiling-Bioluminescence Resonance Energy Transfer Platform Technology Enables Target Engagement Studies with Absolute Specificity in Living Systems

Punita Bathla,[‖] Aaiyas Mujawar,[‖] Abhijit De,* and Britto S. Sandanaraj*

Cite This: *ACS Pharmacol. Transl. Sci.* 2024, 7, 375−383

Read Online

ACCESS | Metrics & More | Article Recommendations | Supporting Information

ABSTRACT: Noninvasive, real-time, longitudinal imaging of protein functions in living systems with unprecedented specificity is one of the critical challenges of modern biomedical research. Toward that goal, here, we report a platform fusion technology called activity-based protein profiling-bioluminescence resonance energy transfer (ABPP-BRET). This method provides an opportunity to study the post-translational modification of a target protein in real time in living systems in a longitudinal manner. This semisynthetic BRET biosensor method is used for target engagement studies and further for inhibitor profiling in live cells. The simplicity of this method coupled with the critical physical distance-dependent BRET readout turned out to be a powerful method, thus pushing the activity-based protein profiling technology to the next level.

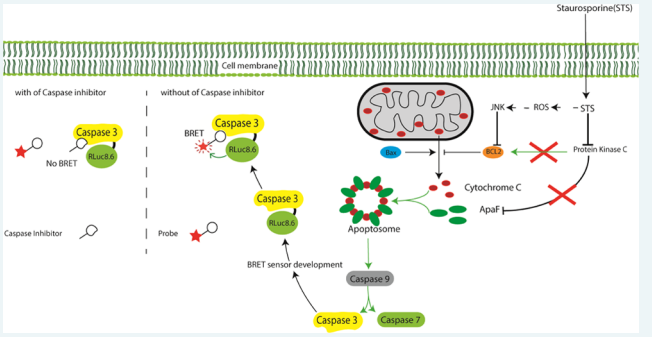

KEYWORDS: *caspase-BRET, caspase activity, caspase activation sensor, caspase-3 activity*

Proteins play a major role in both human physiology and pathology. Despite their critical role, nearly 35% of the human proteome is still not characterized. Out of 65% of proteomes that are characterized, less than 5% of the proteome is focused on drug discovery programs.[1] However, there is renewed interest in studying the entire human proteome in an unbiased manner. The development of new proteomic technologies would greatly facilitate the annotation of the function of a plethora of proteins. In this regard, chemical proteomic technologies have gained a lot of attention in the last two decades.[2,3] In particular, the activity-based protein profiling (ABPP) method has revolutionized the way that we study protein function.[4,5] Currently, this method is widely used for assigning new functions for both known and unknown proteins.[4,5] In addition, this method is widely used in pharmaceuticals/biotech industries and academic laboratories for target identification, target validation, and inhibitor screening.[6−12] The ABPP method uses gel- and/or mass spectrometry (MS)-based detection platforms. The use of gel-based detection is highly attractive because of its simplicity and cost-effective setup. However, the ABPP-gel method suffers from poor resolution and a narrow dynamic range. On the other hand, the MS-based detection method offers superior sensitivity and provides the ability to profile multiple proteins simultaneously in an unbiased manner. Despite these attractive features, the ABPP-MS method suffers from extremely low throughput, which limits parallel and reproducible sample analyses, laborious sample preparation, and the need for large input proteome. Further, the ABPP-MS method requires homogenization of cells/tissues, which results in the loss of spatial information about protein activity both at intra- and intercellular levels.

To address some of the limitations of ABPP-MS, others and we have developed complementary technologies. Moellering group introduced a new method named the "activity-dependent proximity ligation (ADPL)" platform.[13,14] ADPL integrates the use of activity-based probes along with barcoded oligonucleotide proximity ligation and amplification. ADPL offers several advantages, such as (i) direct visualization of "active proteins" with a high spatial resolution, (ii) increased dynamic range through signal amplification, and (iii) deciphering phenotypic heterogeneity in patient tissues. Further, they extended this method for profiling many enzymes simultaneously through multiplexing.[15] The multiplexed activity-based approach was applied to directly quantify small molecule-

Received: September 9, 2023
Revised: December 6, 2023
Accepted: December 18, 2023
Published: January 4, 2024

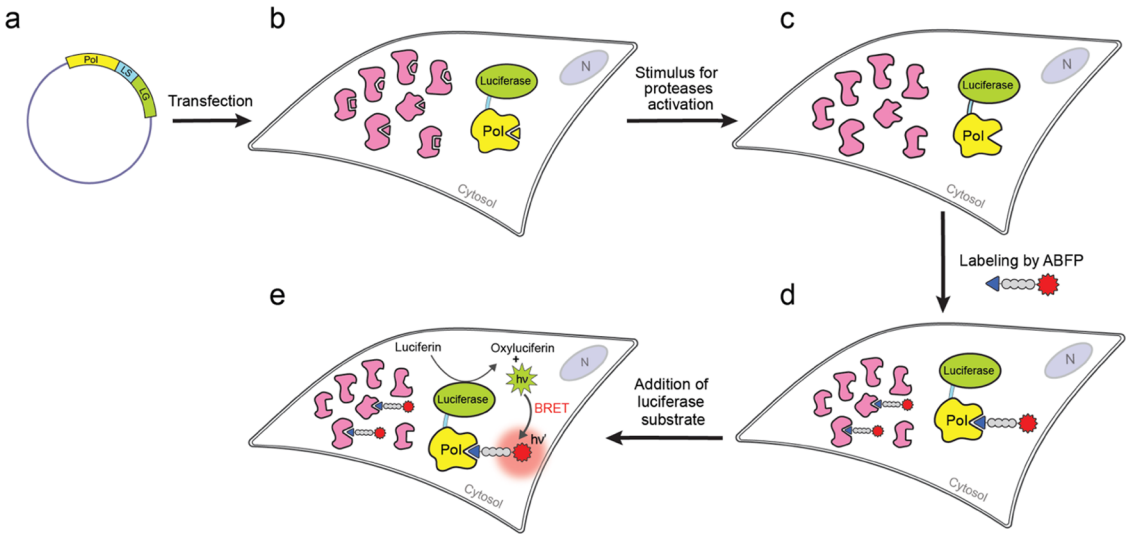

Figure 1. Schematic representation of ABPP-BRET technology. (a) Generation of a plasmid vector encoding for the luciferase tagged to the protease-of-interest (PoI); LS: linker sequence and LG: luciferase gene. Vector encoding the PoI-tagged luciferase is expressed in a suitable cell line. (b) Cells expressing PoI tagged to the luciferase enzyme along with the endogenous protease (pink) of the same or different families. Cells are subjected to an appropriate stimulus for the activation of PoI tagged to luciferase. (c) Cells expressing the active PoI-tagged luciferase and other endogenous proteases. Cells are incubated with an activity-based fluorescent probe (ABFP) with an appropriate warhead and fluorophore. (d) Labeling of the PoI-tagged luciferase enzyme along with other endogenous proteases of the same family by an ABFP. (e) Labeling of PoI by an ABFP creates an instantaneous BRET pair that reports the activity of the PoI.

protein target engagement.[15] Although this method addresses some of the limitations of ABPP-MS, it has several drawbacks, such as (i) it requires fixing and permeabilization of cells, followed by treatment with antibodies labeled with oligonucleotides; (ii) it requires the availability of high-quality primary antibodies that can bind to target proteins with high affinity and specificity; (iii) it is not guaranteed that the epitope region of target protein always be available for antibody recognition as it may be occupied by other biomolecules in the highly complex environment of a living cell; (iv) this method also requires preparation of secondary antibodies labeled with oligonucleotides making it more laborious; and most importantly, (v) this method cannot be used to study the function of active proteins in living systems in real time in a longitudinal manner.

During the same time, our group was also working on the development of complementary technologies to ABPP-MS. We developed a powerful yet simple and easy method named "activity-based reporter gene technology (AbRGT)".[16,17] As the name suggests, this method is the fusion of ABPP with the reporter gene technology. Our technology uses fluorescence resonance energy transfer (FRET) measurement for the detection of protein activity. Using this technology, we demonstrated imaging of active protease in a single live cell in real time with unprecedented specificity. We used this method to study the function of different proteases, such as caspase-3, -7, -8, and -9, in an apoptosis signaling pathway. In addition, for the first time, we investigated the role of cathepsin-B in an apoptosis pathway in a noninvasive manner.[16] Further, this method was used for target engagement studies and inhibitor profiling in live cells. Compared to ABPP-MS and ADPL technologies, ABRGT offers several advantages, such as (i) an extremely simple and powerful method, (ii) protein profiling in live cells with unprecedented specificity, (iii) real-time imaging capabilities, (iv) longitudinal imaging, and (v) in principle could be adopted to study the function of any protein (platform technology). Although extremely powerful, like any other method, this technology also has a few limitations, such as (i) the need for highly sophisticated instruments, such as a confocal microscope, (ii) narrow dynamic range, (iii) low throughput, (iv) the need for highly trained personnel, and (v) most importantly, this technology may not be translated to protein profiling in live animal as FRET study may not be ideal for whole-body imaging experiments.

To address the limitation of our previous method, here, we report a platform technology, named ABPP-BRET. We demonstrate the capability of this method to follow post-translational modification of the caspase-3 enzyme in live cells in real time in a longitudinal way. This method was used for real-time target engagement/inhibitor profiling in live cells by creating a stable cell line expressing the caspase-3-luciferase fusion protein, followed by monitoring of caspase-3 activation upon treatment with a pan-kinase inhibitor. Most importantly, this technology provides opportunities to translate ABPP to study protein function with unprecedented specificity.

The ABPP-BRET method is schematically depicted in Figure 1. Here, the protease-of-interest (PoI) is cloned into a plasmid vector for mammalian expression encoding the luciferase gene, generating a luciferase-tagged PoI recombinant plasmid (Figure 1a). Luciferase-tagged PoI plasmid is expressed in a suitable cell line (Figure 1b). An appropriate stimulus is applied to the cells for the activation of PoI (Figure 1c). Cells were then incubated with an activity-based fluorescent probe (ABFP) for the labeling of PoI (Figure 1d). The choice of ABFP should be such that it allows a significant spectral overlap between its excitation and the emission of luciferase. Subsequently, a specific luciferase substrate is added to the cells. The luciferin substrate will act by luciferase, leading to the generation of photons. As the excitation of ABFP overlaps with the emission spectra of the luciferase substrate, the ABFP gets excited, resulting in the BRET effect (Figure 1e). Since the biophysical principle of the BRET process is proximity-dependent, the efficiency of the

https://doi.org/10.1021/acsptsci.3c00231
ACS Pharmacol. Transl. Sci. 2024, 7, 375−383

transfer of energy is dependent on physical distance between the donor (excited luciferase substrate) and acceptor (ABFP). The nonspecific labeling of other proteases by ABFP in the cell will not interfere with the BRET signal. Thus, the ABPP-BRET method provides opportunities to study the function of the target protein with an unprecedented specificity in live cells in a longitudinal manner.

RESULTS

BRET Pair Selection. BRET assay is highly superior compared to the FRET method because it has a high signal-to-background ratio, as no external light is required; thus, there is no autofluorescence, photobleaching of samples is not an issue, and BRET assay can be used to study kinetics or long-term assay *in vitro* and *in vivo*.[18] Among the various factors, the choice of the donor (luciferase enzyme/substrate pair) and acceptor plays a significant role. We chose FMK-VAD-Rhodamine as an acceptor because this probe is commercially available at a reasonable price. It has been shown to target various cysteine proteases, including caspase (the target protein of our study).[16] Most importantly, the rhodamine emission maxima is around 590 nm, highly suited for *in vivo* BRET-based imaging applications. We chose RLuc 8.6 as a donor because this mutant luciferase has cofactor-independent activity, high photon output, and red-shifted emission.[19] RLuc 8.6 uses coelenterazine h as a substrate, emitting at 535 nm.[19] Most importantly, the emission of coelentrazine h overlaps well with the absorption spectrum of rhodamine dye, an essential prerequisite for an efficient BRET process.

To obtain the RLuc 8.6 emission spectrum, MCF-7 cells were transiently transfected with the RLuc 8.6 plasmid. After 24 h of transfection, the substrate coelenterazine h was added to the cells. Immediately after substrate addition, the emission from coelenterazine was recorded. The emission maxima for coelenterazine h were observed around 520−540 nm, consistent with the previous reports.[19] Afterward, the absorption and emission spectra of rhodamine were acquired. We diluted the Rh-VAD-FMK probe in 1× phosphate-buffered saline (PBS) (Rh-VAD-FMK probe: 1× PBS, 1:500 μL) and excited from 500 to 700 nm. The absorption maximum of rhodamine was observed at 561 nm, which is similar to the reported values. The coelenterazine h and rhodamine spectrum values were normalized and merged to evaluate the spectral overlapping between the coelenterazine h emission and the rhodamine excitation (Figure 2). A significant spectral overlap (540−600 nm) between coelenterazine h and rhodamine establishes RLuc 8.6 and rhodamine as suitable BRET pairs.

Cloning and Expression of Caspase-3-GGS-RLuc 8.6 Fusion Protein in MCF-7 Cells. To develop the BRET-ABPP, we chose caspase-3 as our protein of interest (PoI), as we have already demonstrated the caspase-3 activation via the FRET approach of ABPP.[16,17] Using suitable primers (Supporting Table S1), the human caspase-3 gene was amplified by the polymerase chain reaction (PCR) from pCMV3-C-OFPspark. The amplified caspase-3 gene was digested with restriction enzymes Hind III and *Bgl*II. The digested caspase-3 gene was cloned into the pCMV-GGS-RLuc 8.6 vectors between the Hind III and *Bgl*II restriction sites using the PCR-dependent restriction enzyme-based cloning method.[20] The resultant caspase-3-GGS-RLuc 8.6 clone was confirmed by restriction digestion. We digested the suspected caspase-3-GGS-RLuc 8.6 plasmid with Hind III and *Bgl*II restriction enzymes, as the caspase-3 gene would be incorporated between these sites after ligation. After digestion, the caspase-3 gene would be digested and gave a fallout of around 850 bp (Figure 3a). We further confirmed the proper alignment and ligation of the caspase-3 gene in the GGS-RLuc 8.6 plasmid by carrying out DNA sequencing (Supporting Figures S3−S7).

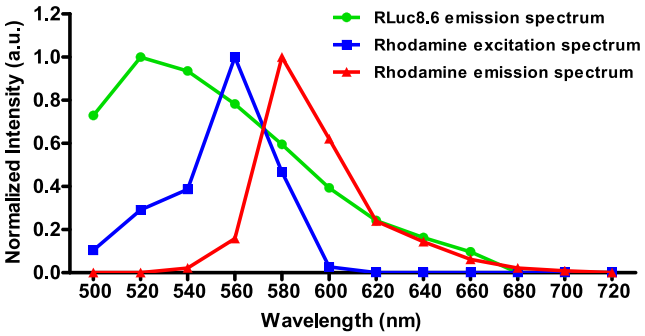

Figure 2. Spectral overlap between the normalized RLuc 8.6 emission spectra and the normalized excitation and emission spectra of the rhodamine dye. RLuc 8.6 is excited by the addition of the substrate, coelenterazine h, and the bioluminescence emission spectrum is recorded (green line). Rhodamine is excited with a 561 nm laser (blue line), and the emission spectra are recorded (red line). RLuc and rhodamine spectra are obtained separately using suitable filter combinations and merged to evaluate the spectral overlapping between the RLuc emission and rhodamine excitation and emission.

The expression of the recombinant caspase-3-GGS-RLuc 8.6 fusion protein was determined by transiently transfecting MCF-7 cells with the pCMV-caspase-3-GGS-RLuc 8.6 plasmid. The transfected cells and control cells (untransfected) were seeded in a 96-black well plate (20,000 cells/well) and incubated for 24 h at suitable conditions, followed by the addition of coelenterazine h. Immediately after coelenterazine h addition, the average radiance was recorded for both the untransfected and pCMV-caspase-3-GGS-RLuc 8.6-transfected MCF-7 cells. The average radiance values for the caspase-3-GGS-RLuc 8.6 transfected cells (5.9×10^5 photons/s/cm^2/sr) are significantly higher as compared to the untransfected cells (2.6×10^3 photons/s/cm^2/sr), confirming that the expression of the recombinant caspase-3-GGS-RLuc 8.6 protein in transfected MCF-7 cells (Figure 3b).

Monitoring of Real-Time Activation of Caspase-3 in Live Cells and Target Engagement Studies. To demonstrate the uniqueness of the ABPP-BRET method, we chose to study the activation of the caspase-3 enzyme in the MCF-7 cell line because it lacks an endogenous caspase-3 enzyme.[21] The transfected MCF-7 cells were treated with staurosporine (STS, pan-kinase inhibitor) (1 μM) for 4 h for the induction of apoptosis.[22,23] The STS triggers apoptosis via the intrinsic pathway and leads to the activation of caspases. Subsequently, cells were incubated with the ABFP−Rh-VAD-FMK probe (BRET acceptor) for the labeling of PoI and other proteases of the same family. The Rh-VAD-FMK probe was chosen because it has been previously shown that this probe labels caspase-3 with low selectivity,[24,25] thus avoiding excessive engineering of ABFP probes. The RLuc 8.6 substrate, coelenterazine h, was added to the cells, and the average radiance was recorded in the donor emission channel and the acceptor emission channel. The BRET measurements were calculated using the mBRET values for the STS-treated versus untreated samples.[26] The calculated mBRET value for the STS-treated sample is 60, which is significantly higher than that

https://doi.org/10.1021/acsptsci.3c00231
ACS Pharmacol. Transl. Sci. 2024, 7, 375−383

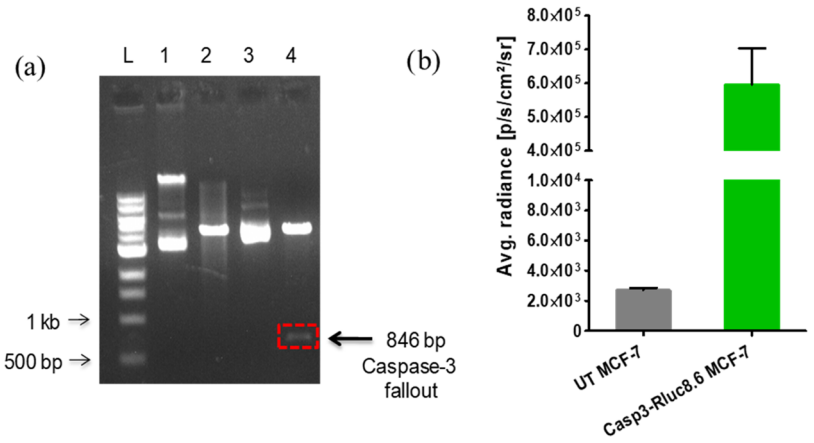

Figure 3. (a) Recombinant pCMV-GGS-RLuc 8.6-caspase-3 plasmid was confirmed by restriction digestion analysis using Hind III and *Bgl*II lane L, 1 kb DNA ladder; lane 1, undigested pCMV-GGS-RLuc 8.6 plasmid; lane 2, pCMV-GGS-RLuc 8.6 plasmid digested with Hind III and *Bgl*II; lane 3, undigested recombinant plasmid pCMV-GGS-RLuc 8.6-caspase-3; lane 4, recombinant pCMV-GGS-RLuc 8.6-caspase-3 plasmid digested with Hind III and *Bgl*II. (b) Expression of recombinant RLuc 8.6-GGS-caspase-3 fusion protein (Casp3-RLuc 8.6) was determined by quantifying the bioluminescence. The bar graph represents the average radiance [p/s/cm^2/sr] for untransfected (UT) MCF-7 cells and transfected MCF-7 cells.

for the untreated control, 11 ± 9 (Figure 4a). This increase in mBRET values in the treated samples indirectly reports real-time activation of the caspase-3 enzyme in live cells.

Overactivation of caspase-3 leads to several acute neurological diseases, such as Huntington's disease,[27] Parkinson's disease,[28] Alzheimer's disease,[29] etc. The inhibitors that are capable of blocking caspase-3 activity would be potential drug candidates and hence beneficial for screening drug targets.[30,31] To check the effect of the caspase inhibitor on the BRET signal, we treated MCF-7 cells expressing the caspase-3-GGS-RLuc 8.6 fusion protein with 4000 nM STS and one group with 4000 nM STS and 1 mM Z-VAD-FMK (caspase inhibitor)[32] for 1 h and then both groups were treated with the ABPP-BRET probe for 1 h. The inhibitor group showed reduced BRET compared to the STS-treated group (Figure 4b) and no significant change compared to vehicle control. Further, to check the effect of increasing concentrations of STS on caspase activation, we treated MCF-7 cells expressing the caspase-3-GGS-RLuc 8.6 fusion protein with increasing concentrations of STS for 4 h. The transfected cells were treated with 250, 500, 1000, 2000, and 4000 nM STS; the BRET signal was recorded for vehicle control and treatment groups. We observed a dose-dependent increase in mBRET values in the treatment group with increasing STS concentration with a calculated EC_{50} of 1.25 μM (Figure 4c). This data suggests that the BRET-based approach can be applied to determine the activation as well as inhibition of caspase activity. Thus, we can effectively use the ABPP-BRET method to screen caspase inhibitors and activators.

Developing a robust screening platform is extremely important for drug discovery programs. Many drugs fail during various phases of clinical trials due to a lack of efficacy. This failure is attributed to a lack of robustness in screening platforms that can select true lead molecules. Therefore, developing a robust, highly sensitive screening method that can provide absolute specificity is highly desired. Toward that goal, here, we demonstrate the application of ABPP-BRET as an excellent screening platform. For inhibitor screening, caspase-3-GGS-RLuc 8.6 expressing MCF-7 cells were treated with STS (1 μM) for 4 h. Subsequently, after STS treatment, cells were incubated with Z-VAD-FMK or caspase inhibitor I, E64, or Q-VD-OPH at two different concentrations (25 or 50 μM) for 1 h. These compounds were selected as they inhibit caspase-3, other caspases, and cysteine proteases.[32−35] Cells were treated with the Rh-VAD-FMK probe for 1 h, followed by the addition of coelenterazine h. Immediately after coelenterazine h addition, the BRET signal was recorded. In the absence of an inhibitor, the calculated mBRET value of the sample was 60 ± 0.4. The inhibition was seen at 50 μM concentration by all inhibitors, but the maximum inhibition was shown by the Q-VD-OPh inhibitor, which was reported as a potent caspase-3 inhibitor.[35] The ABPP-BRET assay also showed mBRET values for the Q-VD-OPh inhibitor as the lowest when compared to the Z-VAD-FMK inhibitor, caspase inhibitor I, and E64 inhibitor (Q-VD-OPh > Z-VAD-FMK > caspase inhibitor I > E64 (Figure 4d)). The above result indicates that the ABPP-BRET method can be used to measure qualitative inhibition of caspase-3 activity.

Demonstration of ABPP-BRET in Stable Cells. The transient transfection method is a straightforward method for introducing a foreign gene into mammalian cells. However, this method has several drawbacks, such as the transfected plasmid may be lost during replication and hence may not be suitable for longitudinal or *in vivo* studies. In addition, overexpression of a certain gene may alter the physiology of the cells. Most importantly, this method cannot be used to generate helpful disease models in rodents. Considering these limitations, we thought demonstrating the ABPP-BRET method in stable cells is critical. The stable cells were generated by transfection of plasmid and then selection of clones by selection marker,[36] as explained in the Materials and Methods Section. Three clones were selected, and their bioluminescence efficiency was measured. Clone 1 has shown high bioluminescence and is selected for further studies (Figure 5a). The MCF-7 cells stably expressing caspase-3-GGS-RLuc 8.6 (MCF-7 CR) were treated with PBS, and different concentrations of STS (50, 100, and 200 nM) for 4 h and one group was treated with 200 nM of STS, followed by 1 mM Z-VAD-FMK (caspase inhibitor). Subsequently, cells were incubated with the Rh-VAD-FMK probe for 1 h, followed by the addition of coelenterazine h. Immediately after substrate addition, the BRET signal was recorded, and the mBRET values were calculated and plotted

https://doi.org/10.1021/acsptsci.3c00231
ACS Pharmacol. Transl. Sci. 2024, 7, 375−383

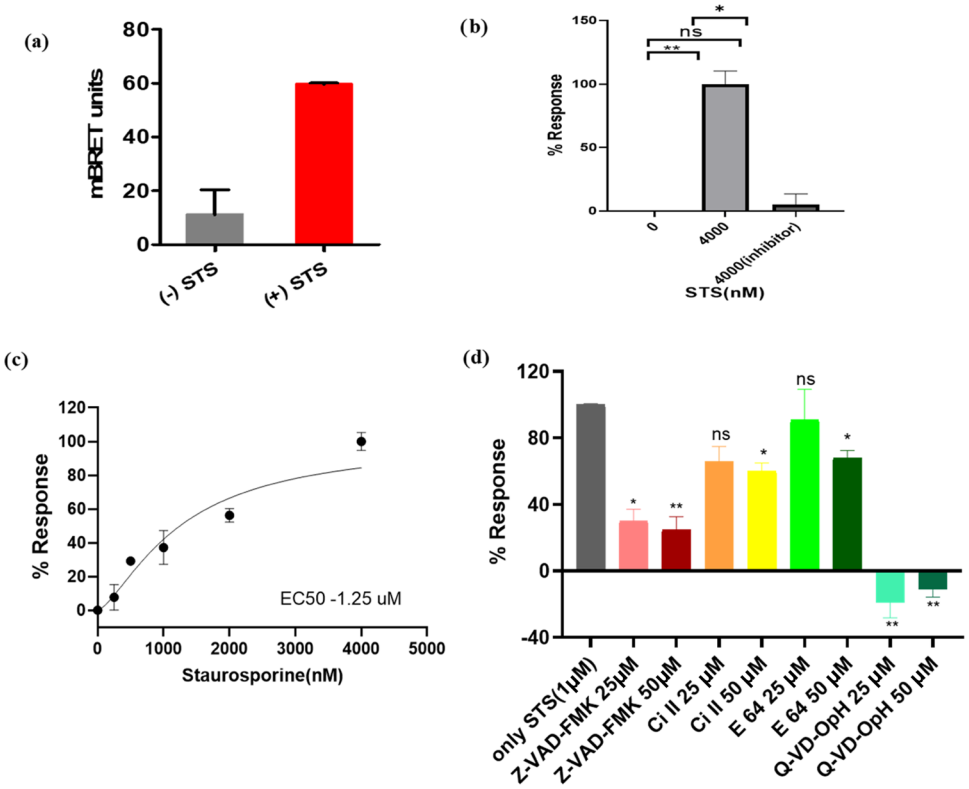

Figure 4. (a) Caspase-3-GGS-RLuc 8.6-transfected MCF-7 cells were treated with or without STS (1 μM) for 4 h. Subsequently, cells were incubated with the Rh-VAD-FMK probe for 1 h, followed by coelenterazine h addition. Immediately after coelenterazine h addition, the average radiance was recorded, and the mBRET values for both the STS-treated and untreated cells were calculated. (b) Caspase-3-GGS-RLuc 8.6-transfected MCF-7 cells were treated without and with STS (4000 nM) for 4 h and one group treated with 4000 nM of STS for 4 h and Z-VAD-FMK (1 mM) for 1 h. Subsequently, cells were incubated with the Rh-VAD-FMK probe for 1 h, followed by coelenterazine h addition. Immediately after coelenterazine h addition, the average radiance was recorded, and the mBRET values for untreated cells and STS-treated cells were calculated and a bar graph was generated. (c) Caspase-3-GGS-RLuc 8.6-transfected MCF-7 cells were treated without and with different concentrations of STS (250−4000 nM) for 4 h. Subsequently, cells were incubated with the Rh-VAD-FMK probe for 1 h, followed by coelenterazine h addition. Immediately after coelenterazine h addition, the average radiance was recorded, and the mBRET values for untreated cells and STS-treated cells were calculated and a dose−response curve was generated. (d) BRET approach of AbRGT for screening inhibitors in a 96-well plate. Caspase-3 RLuc 8.6-transfected MCF-7 cells treated with STS (4 μM) for 4 h. Cells were subsequently treated with different inhibitors, Z-VAD-FMK, caspase Inhibitor I(Ci I), E64, and Q-VD-OPh at concentrations 25 or 50 μM for 1 h. After inhibitor treatment, cells were incubated with the Rh-VAD-FMK probe for 1 h, followed by the substrate coelenterazine h addition. The average radiance was recorded in the acceptor and the donor channel, and the mBRET values are calculated and represented as a bar graph (ns, nonsignificant, *p value <0.05. ** p value >0.01).

as a bar graph (Figure 5b). We found an increase in mBRET values with an increasing STS concentration. An ∼4-fold increase in mBRET was found at 200 nM STS concentration compared to the untreated cells. The addition of a 1 mM Z-VAD-FMK inhibited the activation of caspase-3 and thus abolished the BRET effect (Figure 5b). The above results confirm the occurrence of BRET between RLuc 8.6-coelenterazine h and rhodamine and can be used to study activation or inhibition of caspase-3 activity in stable cells.

DISCUSSION

Even after two decades of the complete human genome draft, we still do not know the function of many proteins. The genomics,[37,38] transcriptomics, and standard proteomics technologies[39,40] have failed to provide information on the function of many proteins. This is mainly attributed to the reason that the function of "active protein" is regulated at multiple levels, such as irreversible post-translational modification[41] and reversible interaction of active proteins with endogenous inhibitors.[42,43] The ABPP-MS method addresses these limitations posed by major "omics" technologies and helps to decipher the function of many proteins, which are involved in many human diseases.[5] ABPP-MS has succeeded as a robust mature technology over the past decade. Because of its unparalleled strength, many academic laboratories and pharmaceutical/biotech industries routinely use ABPP-MS for target identification, target validation, and inhibitor screening.[6−12] However, the existing ABPP-MS method uses fractionated proteomes from cells and tissues for downstream analysis. Because of this limitation, cells and tissues are subjected to sample homogenization and this leads to a loss of spatial information on protein activity.[44,45] In addition, the current ABPP-MS method cannot be used to detect the function of protein directly from living systems in real time in a longitudinal manner.

Considering these limitations, it is important to develop next-generation activity-based chemical proteomics technology, which does not rely on gel- or MS-based detection platforms. With that goal in mind, many research groups are developing complementary technologies. Our group had developed a different version of the activity-based chemical

https://doi.org/10.1021/acsptsci.3c00231
ACS Pharmacol. Transl. Sci. 2024, 7, 375−383

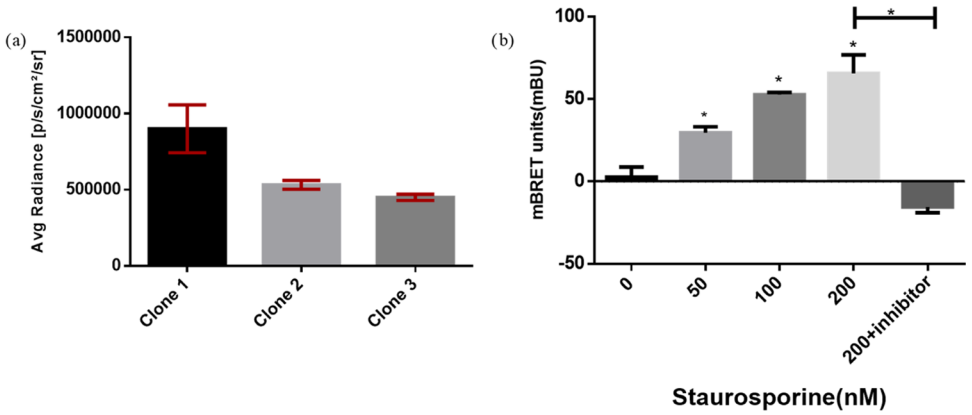

Figure 5. (a) 10,000 cells/well of MCF-7 caspase-3-GGS-RLuc 8.6 clones, clone nos. 1, 2, and 3 were seeded in 96-well plates and incubated for 16 h. After incubation, the RLuc 8.6 substrate, coelenterazine h, was added in each well to measure luciferase activity. The average radiance for clone nos. 1, 2, and 3 was recorded in the open filter and represented as a bar graph. (b) 20,000 cells of clone 1 were seeded in 96-well plates and were treated with increasing concentrations of STS (0, 50, 100, and 200 nM) for 4 h and one of the groups was treated with 200 nM STS, followed by the addition of 1 mM Z-VAD-FMK inhibitor. Subsequently, cells were incubated with the Rh-VAD-FMK probe for 1 h, followed by coelenterazine h addition. Immediately after coelenterazine h addition, the average radiance was recorded, and the mBRET values were calculated and represented as a bar graph (ns, nonsignificant, *p value <0.05).

proteomics method named AbRGT 1.0,[16,17] which utilizes FRET-based readout to detect protein activity. Although powerful, the AbRGT-FRET method has certain limitations and, therefore, reduces the scope of this technology. Therefore, the present study was directed toward preserving superior attributes of activity-based reporter gene technology (AbRGT) while addressing some of the limitations caused by FRET-based measurement and avoiding the use of a highly expensive confocal microscope. To do that, we decided to explore the bioluminescence resonance energy transfer (BRET) technology. The BRET method is currently used for the detection of noninvasive imaging of protein function both in live cells as well as animal or plant models in real time in a longitudinal manner.[46−48] However, most of the previous BRET-based methods lack specificity and therefore produce ambiguous results. The pioneering work by Robers and co-workers addresses the "specificity issue" by developing nanoBRET platforms.[49−51] This method provides unprecedented specificity to study the function of active proteins and can be used for target engagement studies and inhibitor profiling in live cells in real time. Inspired by the work of Robers et al., we would like to develop a technology that can be applied to a large number of proteins by using commercially available, off-the-shelf family-wide fluorescent activity-based probes. To achieve this goal, we decided to combine ABPP with the BRET method to create ABPP-BRET technology. As a proof of concept, we transiently expressed the caspase-3-luciferase enzyme in the MCF-7 cells, followed by treatment with a pan-kinase inhibitor (STS). The treatment of MCF-7 cells with STS leads to proteolytic activation of the caspase-3-luciferase enzyme, followed by labeling of the caspase-3 enzyme of the fusion protein by an FMK-VAD-Rhodamine chemical probe to create an in situ BRET pair. As expected, there was no or negligible BRET before probe addition; however, we observed an increase in BRET value with an increased concentration of STS. To demonstrate that the BRET signal truly comes from the target protein (i.e., caspase-3-luciferase enzyme), we have carried out experiments in the presence of potent caspase inhibitors; as expected, the BRET signal considerably decreased in the presence of various caspase inhibitors. This result manifests that the BRET signal is indeed coming from the target protein. Further, we have utilized this method for target engagement studies with various irreversible and reversible inhibitors. As expected, we obtained different mBRET values depending on the compound's potency. Further, we created an engineered stable MCF-7 cell line expressing the caspase-3 luciferase fusion protein, followed by the demonstration of dose-dependent proteolytic activation of the caspase-3-luciferase enzyme upon treatment with different concentrations of STS.

It is quite evident that these three technologies (ABPP-MS, ADPL, and ABPP-BRET) have their own merits and limitations. For example, ADPL[13−15] and ABPP-BRET cannot be used for target identification in an unbiased manner at the system level, whereas ABPP-MS[6−12] is routinely used for this purpose. Similarly, ABPP-MS and BRET-ABPP cannot be employed for the analysis of patients' samples, whereas ADPL is uniquely suited to do that.[15] ABPP-BRET can be used for profiling proteins in live cells in real time in a longitudinal manner, but the other two technologies do not have that capability. ABPP-MS and ADPL do not involve the genetic engineering of cells and therefore provide the opportunity to look at the activity of endogenous proteins, whereas ABPP-BRET involves the expression of exogenous fusion reporter protein to report endogenous activity from live cells. This method is simple and powerful, but further studies are required to validate its full potential as a quantitative and throughput screening assay for target engagement studies. Therefore, ABPP-BRET technology is not a replacement for the most powerful ABPP-MS or ADPL technologies, whereas it is complementary to the existing technologies. We firmly believe that each of these three technologies complements each other and therefore collectively provides powerful tools to interrogate protein function at the system level.

CONCLUSIONS

In summary, we have introduced a new chemical proteomics technology to the existing toolbox. ABPP-BRET technology provides an opportunity to study the function of the "active enzyme" with unprecedented specificity. In particular, this method allows real-time monitoring of proteolytic activation of the target protein in live cells. We also demonstrated that this

https://doi.org/10.1021/acsptsci.3c00231
ACS Pharmacol. Transl. Sci. 2024, 7, 375−383

method could be used for target engagement studies in live cells in real time. Further, the creation of a stable cell line expressing caspase-3 luciferase offers longitudinal imaging of live cells and opportunities to translate the ABPP technology to follow the function of "active proteins" in live animals in real time in a longitudinal manner with unprecedented specificity.

MATERIALS AND METHODS

Reagents. Lipofectamine 2000, E64 protease inhibitor, Q-VD-OPh hydrate, cpm-VAD-CHO, staurosporine, caspase-3 inhibitor I, and coelentrazine h were procured from Sigma. An Rh-VAD-FMK probe and a Z-VAD-FMK inhibitor were obtained from Abcam.

Cloning. For pCMV-caspase-3-GGS-RLuc 8.6 recombinant vector preparation, 846 bp of the human caspase-3 gene was PCR-amplified from the pCMV3-C-OFPspark plasmid using suitable primers. The amplified 846 bp caspase-3 PCR product was digested with Hind III and *Bgl*II restriction enzymes and cloned into pCMV-GGS-RLuc 8.6 vector between the restriction sites Hind III and *Bgl*II using a PCR-based method for restriction cloning.[20] The clones were confirmed by restriction digestion and DNA sequencing.

Transient Transfections. MCF-7 cells were seeded in a 35 mm dish and were transiently transfected with the pCMV-caspase-3-GGS-RLuc 8.6 recombinant plasmid at 70% cell confluency using Lipofectamine 2000 reagent. Twenty-four hours post-transfection, the cells were trypsinized and distributed in a 96-well black plate with a clear bottom (20,000 cells/well). Cells were allowed to attach by overnight incubation in a humidified atmosphere of 5% CO_2 at 37 °C before the start of experiments.

Luciferase Assay. In transfected MCF-7 seeded in 96-black well plates, the RLuc 8.6 substrate, coelenterazine h (50 μL of the 1 mg/mL stock, dissolved in 1× PBS), was added to each well. Immediately after substrate addition, cells were analyzed in an IVIS spectrum with an emission spectrum (520−540 nm) using an integration time (60 s/filter), and the average radiance for each well was recorded.

Caspase-3 Activity Measurement. For the caspase-3 activity measurements, pCMV-caspase-3-GGS-RLuc 8.6-transfected MCF-7 cells in a 96-black well clear bottom plate were treated with STS (1 μM) for 4 h. Cells were then incubated with the Rh-VAD-FMK probe for an additional 1 h. Subsequently, the RLuc 8.6 substrate, coelenterazine h, was added to the cells, and the average radiance value for each well was taken immediately using an IVIS spectrum at 520−540 nm wavelength as the donor filter and 560−580 nm as the acceptor filter.

Effect of Inhibitor on STS-Based Caspase Activation. The MCF-7 cells transfected with the pCMV-caspase-3-GGS-Rluc8.6 plasmid were seeded in a 96-black well clear bottom plate (20,000 cells/well) and treated with PBS or increasing concentration of STS (250−4000 nM) for 4 h. One group of treated cells was incubated for 1 h with Z-VAD-FMK (50 μM). Both groups were incubated with the ABFP−Rh-VAD-FMK probe for 1 h. The RLuc 8.6 substrate, coelenterazine h, was added to the cells, and the average radiance was recorded in the donor emission channel, RLuc 8.6 (520−540 nm), and the acceptor emission channel, rhodamine (580−600 nm). BRET calculations were performed as described before.

Inhibitors Screening. For inhibitor screening, pCMV-caspase-3-GGS-RLuc 8.6-transfected MCF-7 cells in 96-black well plates with a clear bottom were pretreated with different inhibitors. The treatment of the inhibitors was performed for 1 h before Rh-VAD-FMK probe incubation. Different concentrations of the inhibitors (25 and 50 μM) were tested. Subsequently, caspase-3 labeling was performed by incubation of the cells with the Rh-VAD-FMK probe for 1 h. For BRET studies, coelentrazine h was added to the cells, and immediately after substrate addition, the average radiance was recorded.

Preparation of Stable Clone. The MCF-7 cells were seeded in a 35 mm plate at 70% confluency and subsequently transfected with the pCMV-caspase-3-GGS-RLuc 8.6 plasmid by using Lipofectamine 2000 as per manufacturer's instructions. The transfected cells were incubated for 48 h for the expression of the transfected plasmid. Transfected cells were then grown in RPMI under zeocin (300 μg/mL), an antibiotic selection marker, to allow colony formation from single cells in a 10 cm plate. The plate was incubated until colonies were formed. Colonies formed from single cells were picked up and grown in a 96-well plate. After cells attained confluency in a 96-well plate, they were transferred to a 24-well plate, and then clones were grown in bulk to check the expression of the caspase-3-GGS-Rluc8.6 protein with respect to the luciferase activity of RLuc 8.6. The clones with high luciferase activity were selected for further experiments.

BRET Measurements. To perform the BRET measurements for each sample, the image obtained from the IVIS spectrum was analyzed using Living Image software (version 4.5). The image file was opened, and regions of interest (ROIs) were drawn over each well, and the values of average radiance (photons/sec/cm^2/sr) were obtained. The average radiance values were acquired for the donor channel (donor emission channel, 520−540 nm, RLuc 8.6) and the acceptor channel (acceptor emission channel, 580−600 nm, rhodamine). The acceptor/donor channel emission (A/D) ratio was calculated for the donor (D) only and the donor + acceptor (D + A) sample. The A/D channel emission ratio of the D-only sample was subtracted from the D + A sample to obtain the corrected BRET ratio (cBRET).[26] Subsequently, mBRET values were calculated by multiplying the values of the corrected BRET ratio by 1000. The calculations were done using MS Excel; data were statistically analyzed and represented using Graph Prism software version 6.5.

$$\text{A/D channel emission ratio} = \frac{\text{acceptor channel emission}}{\text{donor channel emission}}$$

$$\text{mBRET ratio} = \frac{\text{acceptor channel emission (D + A)}}{\text{donor channel emission (D + A)}} - \frac{\text{acceptor channel emission (D only)}}{\text{donor channel emission (D only)}}$$

$$\text{mBRET unit} = \text{cBRET ratio} \times 1000$$

Statistical Analysis. All *in vitro* data comparisons were done using Welch's modification Student's *t*-test by using GraphPad prism, unless otherwise stated. Error bars represent the standard error of the mean (SEM) from at least three independent experiments. Values of $p < 0.05$ were considered as statistically significant.

https://doi.org/10.1021/acsptsci.3c00231
ACS Pharmacol. Transl. Sci. 2024, 7, 375−383

■ ASSOCIATED CONTENT

Supporting Information

The Supporting Information is available free of charge at https://pubs.acs.org/doi/10.1021/acsptsci.3c00231.

Data for subcloning of the pCMV-caspase-3-GGS-RLuc 8.6 plasmid and structural information on caspases inhibitors; sequence of primers used in cloning (Table S1); standardization of PCR thermocycler conditions for amplification of caspase-3 gene (Table S2); caspase inhibitors used in the study (Table S3); agarose gel image of PCR amplicon from different annealing temperatures (Figure S1); gel image of restriction digestion of pCMV-GGS-RLuc 8.6 (Figure S2); agarose gel electrophoresis image of colony PCR done of transformants (Figure S3); agarose gel electrophoresis image of digestion of selected positive colonies (Figure S4); nucleotide blast result of plasmid caspase-3-GGS-RLuc 8.6 with caspase-3 gene (Figure S5); plasmid map of pCMV-Caspase-3-GGS-RLuc 8.6 (Figure S6); gel of colony PCR done of transformants from ligation (Figure S7); and structure of caspase inhibitors (Figure S8) (PDF)

■ AUTHOR INFORMATION

Corresponding Authors

Abhijit De − *Molecular Functional Imaging Lab, Advanced Centre for Treatment Research Education in Cancer (ACTREC), Navi Mumbai 410210, India; Homi Bhabha National Institute, Mumbai 400094, India;* orcid.org/0000-0002-5818-0206; Email: ade@actrec.gov.in

Britto S. Sandanaraj − *Department of Biology, Department of Chemistry, Indian Institute of Science Education and Research, Pune 411008, India;* orcid.org/0000-0001-8433-2704; Email: sandanaraj.britto@iiserpune.ac.in

Authors

Punita Bathla − *Department of Biology, Department of Chemistry, Indian Institute of Science Education and Research, Pune 411008, India*

Aaiyas Mujawar − *Molecular Functional Imaging Lab, Advanced Centre for Treatment Research Education in Cancer (ACTREC), Navi Mumbai 410210, India; Homi Bhabha National Institute, Mumbai 400094, India*

Complete contact information is available at: https://pubs.acs.org/10.1021/acsptsci.3c00231

Author Contributions

‖P.B. and A.M. are contributed equally to the work. P.B. and A.M. carried out the subcloning and screening for the pCMV-caspase-3-GGS-RLuc 8.6 plasmid and all of the cell culture and associated experiments. A.D. and B.S.S. are responsible for study design, supervision, project administration, and funding acquisition.

Notes

The authors declare the following competing financial interest(s): We have filed both Indian/US patents for the technology disclosed in this paper.

■ ACKNOWLEDGMENTS

This work was supported by DST-SERB Early Career Award to B.S.S., DST-SERB (ECR/2015/000253), and the DBT grant (BT/PRI1450/BRB/I0/1370/2015).

■ REFERENCES

(1) Müller, S.; Ackloo, S.; Al Chawaf, A.; Al-Lazikani, B.; Antolin, A.; Baell, J. B.; Beck, H.; Beedie, S.; Betz, U. A. K.; Bezerra, G. A.; Brennan, P. E.; Brown, D.; Brown, P. J.; Bullock, A. N.; Carter, A. J.; Chaikuad, A.; Chaineau, M.; Ciulli, A.; Collins, I.; Dreher, J.; Drewry, D.; Edfeldt, K.; Edwards, A. M.; Egner, U.; Frye, S. V.; Fuchs, S. M.; Hall, M. D.; Hartung, I. V.; Hillisch, A.; Hitchcock, S. H.; Homan, E.; Kannan, N.; Kiefer, J. R.; Knapp, S.; Kostic, M.; Kubicek, S.; Leach, A. R.; Lindemann, S.; Marsden, B. D.; Matsui, H.; Meier, J. L.; Merk, D.; Michel, M.; Morgan, M. R.; Mueller-Fahrnow, A.; Owen, D. R.; Perry, B. G.; Rosenberg, S. H.; Saikatendu, K. S.; Schapira, M.; Scholten, C.; Sharma, S.; Simeonov, A.; Sundström, M.; Superti-Furga, G.; Todd, M. H.; Tredup, C.; Vedadi, M.; Von Delft, F.; Willson, T. M.; Winter, G. E.; Workman, P.; Arrowsmith, C. H. Target 2035 − Update on the Quest for a Probe for Every Protein. *RSC Med. Chem.* **2022**, *13* (1), 13−21.

(2) Cravatt, B. F.; Sorensen, E. J. Chemical Strategies for the Global Analysis of Protein Function. *Curr. Opin. Chem. Biol.* **2000**, *4* (6), 663−668.

(3) Speers, A. E.; Cravatt, B. F. Chemical Strategies for Activity-Based Proteomics. *ChemBioChem* **2004**, *5* (1), 41−47.

(4) Saghatelian, A.; Cravatt, B. F. Assignment of Protein Function in the Postgenomic Era. *Nat. Chem. Biol.* **2005**, *1* (3), 130−142.

(5) Barglow, K. T.; Cravatt, B. F. Activity-Based Protein Profiling for the Functional Annotation of Enzymes. *Nat. Methods* **2007**, *4* (10), 822−827.

(6) Cisar, J. S.; Cravatt, B. F. Fully Functionalized Small-Molecule Probes for Integrated Phenotypic Screening and Target Identification. *J. Am. Chem. Soc.* **2012**, *134* (25), 10385−10388.

(7) Simon, G. M.; Niphakis, M. J.; Cravatt, B. F. Determining Target Engagement in Living Systems. *Nat. Chem. Biol.* **2013**, *9* (4), 200−205.

(8) Niphakis, M. J.; Cravatt, B. F. Enzyme Inhibitor Discovery by Activity-Based Protein Profiling. *Annu. Rev. Biochem.* **2014**, *83*, 341−377.

(9) Arastu-Kapur, S.; Ponder, E. L.; Fonović, U. P.; Yeoh, S.; Yuan, F.; Fonović, M.; Grainger, M.; Phillips, C. I.; Powers, J. C.; Bogyo, M. Identification of Proteases That Regulate Erythrocyte Rupture by the Malaria Parasite Plasmodium Falciparum. *Nat. Chem. Biol.* **2008**, *4* (3), 203−213.

(10) Bachovchin, D. A.; Brown, S. J.; Rosen, H.; Cravatt, B. F. Identification of Selective Inhibitors of Uncharacterized Enzymes by High-Throughput Screening with Fluorescent Activity-Based Probes. *Nat. Biotechnol.* **2009**, *27* (4), 387−394.

(11) Bachovchin, D. A.; Ji, T.; Li, W.; Simon, G. M.; Blankman, J. L.; Adibekian, A.; Hoover, H.; Niessen, S.; Cravatt, B. F. Superfamily-Wide Portrait of Serine Hydrolase Inhibition Achieved by Library-versus-Library Screening. *Proc. Natl. Acad. Sci. U.S.A.* **2010**, *107* (49), 20941−20946.

(12) Li, W.; Blankman, J. L.; Cravatt, B. F. A Functional Proteomic Strategy to Discover Inhibitors for Uncharacterized Hydrolases. *J. Am. Chem. Soc.* **2007**, *129* (31), 9594−9595.

(13) Li, G.; Montgomery, J. E.; Eckert, M. A.; Chang, J. W.; Tienda, S. M.; Lengyel, E.; Moellering, R. E. An Activity-Dependent Proximity Ligation Platform for Spatially Resolved Quantification of Active Enzymes in Single Cells. *Nat. Commun.* **2017**, *8* (1), No. 1775.

(14) Li, G.; Moellering, R. E. Chemical Probes for Spatially Resolved Measurement of Active Enzymes in Single Cells. *Methods Enzymol.* **2019**, *628*, 243−262.

(15) Li, G.; Eckert, M. A.; Chang, J. W.; Montgomery, J. E.; Chryplewicz, A.; Lengyel, E.; Moellering, R. E. Ultrasensitive, Multiplexed Chemoproteomic Profiling with Soluble Activity-Dependent Proximity Ligation. *Proc. Natl. Acad. Sci. U.S.A.* **2019**, *116* (43), 21493−21500.

(16) Bathla, P.; Sandanaraj, B. S. Development of Activity-Based Reporter Gene Technology for Imaging of Protease Activity with an Exquisite Specificity in a Single Live Cell. *ACS Chem. Biol.* **2019**, *14* (10), 2276−2285.

(17) Britto, S. S.; Bathla, P. Process for determining enzyme activity in a cell by activity-based reporter gene technology (ABRGT). U.S. Patent, US11,834,698A12023.
(18) De, A.; Ray, P.; Loening, A. M.; Gambhir, S. S. BRET3: A Red-shifted Bioluminescence Resonance Energy Transfer (BRET)-based Integrated Platform for Imaging Protein-protein Interactions from Single Live Cells and Living Animals. *FASEB J.* **2009**, *23* (8), 2702−2709.
(19) Dragulescu-Andrasi, A.; Chan, C. T.; De, A.; Massoud, T. F.; Gambhir, S. S. Bioluminescence Resonance Energy Transfer (BRET) Imaging of Protein-Protein Interactions within Deep Tissues of Living Subjects. *Proc. Natl. Acad. Sci. U.S.A.* **2011**, *108* (29), 12060−12065.
(20) Hoseini, S. S.; Sauer, M. G. Molecular Cloning Using Polymerase Chain Reaction, an Educational Guide for Cellular Engineering. *J. Biol. Eng.* **2015**, *9* (1), No. 2.
(21) Jänicke, R. U.; Sprengart, M. L.; Wati, M. R.; Porter, A. G. Caspase-3 Is Required for DNA Fragmentation and Morphological Changes Associated with Apoptosis. *J. Biol. Chem.* **1998**, *273* (16), 9357−9360.
(22) Bertrand, R.; Solary, E.; O'Connor, P.; Kohn, K. W.; Pommier, Y. Induction of a Common Pathway of Apoptosis by Staurosporine. *Exp. Cell Res.* **1994**, *211* (2), 314−321.
(23) Jacobsen, M. D.; Weil, M.; Raff, M. C. Role of Ced-3/ICE-Family Proteases in Staurosporine-Induced Programmed Cell Death. *J. Cell Biol.* **1996**, *133* (5), 1041−1051.
(24) Berger, A. B.; Sexton, K. B.; Bogyo, M. Commonly Used Caspase Inhibitors Designed Based on Substrate Specificity Profiles Lack Selectivity. *Cell Res.* **2006**, *16* (12), 961−963.
(25) Deshmukh, M. Caspases in Ischaemic Brain Injury and Neurodegenerative Disease. *Apoptosis* **1998**, *3* (6), 387−394.
(26) Rathod, M.; Mal, A.; De, A. Reporter-Based BRET Sensors for Measuring Biological Functions in Vivo. In *Methods in Molecular Biology*; Humana Press Inc., 2018; Vol. *1790*, pp 51−74.
(27) Toulmond, S.; Tang, K.; Bureau, Y.; Ashdown, H.; Degen, S.; O'Donnell, R.; Tam, J.; Han, Y.; Colucci, J.; Giroux, A.; Zhu, Y.; Boucher, M.; Pikounis, B.; Xanthoudakis, S.; Roy, S.; Rigby, M.; Zamboni, R.; Robertson, G. S.; Ng, G. Y. K.; Nicholson, D. W.; Flückiger, J. P. Neuroprotective Effects of M826, a Reversible Caspase-3 Inhibitor, in the Rat Malonate Model of Huntington's Disease. *Br. J. Pharmacol.* **2004**, *141* (4), 689−697.
(28) Hartmann, A.; Hunot, S.; Michel, P. P.; Muriel, M. P.; Vyas, S.; Faucheux, B. A.; Mouatt-Prigent, A.; Turmel, H.; Srinivasan, A.; Ruberg, M.; Evan, G. I.; Agid, Y.; Hirsch, E. C. Caspase-3: A Vulnerability Factor and Final Effector in Apoptotic Death of Dopaminergic Neurons in Parkinson's Disease. *Proc. Natl. Acad. Sci. U.S.A.* **2000**, *97* (6), 2875−2880.
(29) Louneva, N.; Cohen, J. W.; Han, L. Y.; Talbot, K.; Wilson, R. S.; Bennett, D. A.; Trojanowski, J. Q.; Arnold, S. E. Caspase-3 Is Enriched in Postsynaptic Densities and Increased in Alzheimer's Disease. *Am. J. Pathol.* **2008**, *173* (5), 1488−1495.
(30) Himi, T.; Ishizaki, Y.; Murota, S. I. A Caspase Inhibitor Blocks Ischaemia-Induced Delayed Neuronal Death in the Gerbil. *Eur. J. Neurosci.* **1998**, *10* (2), 777−781.
(31) Li, H.; Colbourne, F.; Sun, P.; Zhao, Z.; Buchan, A. M. Caspase Inhibitors Reduce Neuronal Injury after Focal but Not Global Cerebral Ischemia in Rats. *Stroke* **2000**, *31* (1), 176−182.
(32) Slee, E. A.; Zhu, H.; Chow, S. C.; MacFarlane, M.; Nicholson, D. W.; Cohen, G. M. Benzyloxycarbonyl-Val-Ala-Asp (OMe) Fluoromethylketone (Z-VAD.FMK) Inhibits Apoptosis by Blocking the Processing of CPP32. *Biochem. J.* **1996**, *315* (Pt 1), 21−24.
(33) Hanada, K.; Tamai, M.; Yamagishi, M.; Ohmura, S.; Sawada, L.; Tanaka, I. Isolation and Characterization of E−64, a New Thiol Protease Inhibitor. *Agric. Biol. Chem.* **2014**, *42* (3), 523−528.
(34) Barrett, A. J.; Kembhavi, A. A.; Brown, M. A.; Kirschke, H.; Knight, C. G.; Tamai, M.; Hanada, K. L-Trans-Epoxysuccinyl-Leucylamido(4-Guanidino)Butane (E-64) and Its Analogues as Inhibitors of Cysteine Proteinases Including Cathepsins B, H and L. *Biochem. J.* **1982**, *201* (1), 189−198.
(35) Caserta, T. M.; Smith, A. N.; Gultice, A. D.; Reedy, M. A.; Brown, T. L. Q-VD-OPh, a Broad Spectrum Caspase Inhibitor with Potent Antiapoptotic Properties. *Apoptosis* **2003**, *8* (4), 345−352.
(36) Wurm, F. M. Production of Recombinant Protein Therapeutics in Cultivated Mammalian Cells. *Nat. Biotechnol.* **2004**, *22* (11), 1393−1398.
(37) Schena, M.; Heller, R. A.; Theriault, T. P.; Konrad, K.; Lachenmeier, E.; Davis, R. W. Microarrays: Biotechnology's Discovery Platform for Functional Genomics. *Trends Biotechnol.* **1998**, *16* (7), 301−306.
(38) Lockhart, D. J.; Winzeler, E. A. Genomics, Gene Expression and DNA Arrays. *Nature* **2000**, *405* (6788), 827−836.
(39) Anderson, N. L.; Anderson, N. G. Proteome and Proteomics: New Technologies, New Concepts, and New Words. *Electrophoresis* **1998**, *19* (11), 1853−1861.
(40) Pandey, A.; Mann, M. Proteomics to Study Genes and Genomes. *Nature* **2000**, *405* (6788), 837−846.
(41) Khan, A. R.; James, M. N. G. Molecular Mechanisms for the Conversion of Zymogens to Active Proteolytic Enzymes. *Protein Sci.* **1998**, *7* (4), 815−836.
(42) Whisstock, J.; Skinner, R.; Lesk, A. M. An Atlas of Serpin Conformations. *Trends Biochem. Sci.* **1998**, *23* (2), 63−67.
(43) Roberts, R. M.; Mathialagan, N.; Duffy, J. Y.; Smith, G. W. Regulation and Regulatory Role of Proteinase Inhibitors. *Crit. Rev. Eukaryotic Gene Expression* **1995**, *5* (3−4), 385−436.
(44) Schürmann, M.; Janning, P.; Ziegler, S.; Waldmann, H. Small-Molecule Target Engagement in Cells. *Cell Chem. Biol.* **2016**, *23* (4), 435−441.
(45) Schirle, M.; Bantscheff, M.; Kuster, B. Mass Spectrometry-Based Proteomics in Preclinical Drug Discovery. *Chem. Biol.* **2012**, *19* (1), 72−84.
(46) Massoud, T. F.; Gambhir, S. S. Molecular Imaging in Living Subjects: Seeing Fundamental Biological Processes in a New Light. *Genes Dev.* **2003**, *17*, 545−580.
(47) Wu, J. C.; Inubushi, M.; Sundaresan, G.; Schelbert, H. R.; Gambhir, S. S. Optical Imaging of Cardiac Reporter Gene Expression in Living Rats. *Circulation* **2002**, *105* (14), 1631−1634.
(48) Ray, P.; Pimenta, H.; Paulmurugan, R.; Berger, F.; Phelps, M. E.; Iyer, M.; Gambhir, S. S. Noninvasive Quantitative Imaging of Protein-Protein Interactions in Living Subjects. *Proc. Natl. Acad. Sci. U.S.A.* **2002**, *99* (5), 3105−3110.
(49) Robers, M. B.; Dart, M. L.; Woodroofe, C. C.; Zimprich, C. A.; Kirkland, T. A.; Machleidt, T.; Kupcho, K. R.; Levin, S.; Hartnett, J. R.; Zimmerman, K.; Niles, A. L.; Ohana, R. F.; Daniels, D. L.; Slater, M.; Wood, M. G.; Cong, M.; Cheng, Y.; Wood, K. V. Target Engagement and Drug Residence Time Can Be Observed in Living Cells with BRET. *Nat. Commun.* **2015**, *6*, No. 10091.
(50) Vasta, J. D.; Corona, C. R.; Wilkinson, J.; Zimprich, C. A.; Hartnett, J. R.; Ingold, M. R.; Zimmerman, K.; Machleidt, T.; Kirkland, T. A.; Huwiler, K. G.; Ohana, R. F.; Slater, M.; Otto, P.; Cong, M.; Wells, C. I.; Berger, B. T.; Hanke, T.; Glas, C.; Ding, K.; Drewry, D. H.; Huber, K. V. M.; Willson, T. M.; Knapp, S.; Müller, S.; Meisenheimer, P. L.; Fan, F.; Wood, K. V.; Robers, M. B. Quantitative, Wide-Spectrum Kinase Profiling in Live Cells for Assessing the Effect of Cellular ATP on Target Engagement. *Cell Chem. Biol.* **2018**, *25* (2), 206−214.e11.
(51) Robers, M. B.; Vasta, J. D.; Corona, C. R.; Ohana, R. F.; Hurst, R.; Jhala, M. A.; Comess, K. M.; Wood, K. V. Quantitative, Real-Time Measurements of Intracellular Target Engagement Using Energy Transfer. *Methods Mol. Biol.* **2019**, *1888*, 45−71.

https://doi.org/10.1021/acsptsci.3c00231
ACS Pharmacol. Transl. Sci. 2024, 7, 375−383